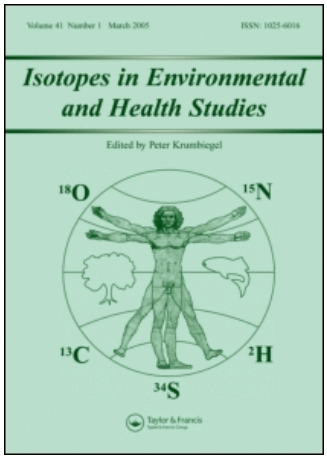

Isotopes in Environmental and Health Studies
Publication details, including instructions for authors and subscription information:
http://www.informaworld.com/smpp/title~content=t713643233

Evaporative isotope enrichment as a constraint on reach water balance along a dryland river

John J. Gibson [ab]; Mostafa A. Sadek [ac]; D. J. M. Stone [a]; Catherine E. Hughes [a]; S. Hankin [a]; Dioni I. Cendon [a]; Suzanne E. Hollins [a]
[a] Australian Nuclear Science and Technology Organization, NSW, Australia
[b] Alberta Research Council, c/o University of Victoria, Geography, Victoria, BC, Canada
[c] Atomic Energy Authority, Cairo, Egypt

Online Publication Date: 01 March 2008

To cite this Article: Gibson, John J., Sadek, Mostafa A., Stone, D. J. M., Hughes, Catherine E., Hankin, S., Cendon, Dioni I. and Hollins, Suzanne E. (2008) 'Evaporative isotope enrichment as a constraint on reach water balance along a dryland river', Isotopes in Environmental and Health Studies, 44:1, 83 — 98

To link to this article: DOI: 10.1080/10256010801887489
URL: http://dx.doi.org/10.1080/10256010801887489

Isotopes in Environmental and Health Studies
Vol. 44, No. 1, March 2008, 83–98

Taylor & Francis
Taylor & Francis Group

Evaporative isotope enrichment as a constraint on reach water balance along a dryland river

JOHN J. GIBSON*†‡, MOSTAFA A. SADEK†§, D.J.M. STONE†, CATHERINE E. HUGHES†, S. HANKIN†, DIONI I. CENDON† and SUZANNE E. HOLLINS†

†Australian Nuclear Science and Technology Organization, PMB 1 Menai, NSW 2234, Australia
‡Alberta Research Council, c/o University of Victoria, Geography, PO Box 3050 STN CSC, Victoria, BC, Canada V8W 3P5
§Atomic Energy Authority, 3 Ahmed El-Zomor St., Nasr City, 11762 Cairo, Egypt

(Received 27 July 2007; in final form 08 November 2007)

Deuterium and oxygen-18 enrichment in river water during its transit across dryland region is found to occur systematically along evaporation lines with slopes of close to 4 in ^{2}H–^{18}O space, largely consistent with trends predicted by the Craig–Gordon model for an open-water dominated evaporating system. This, in combination with reach balance assessments and derived runoff ratios, strongly suggests that the enrichment signal and its variability in the Barwon–Darling river, Southeastern Australia is acquired during the process of evaporation from the river channel itself, as enhanced by the presence of abundant weirs, dams and other storages, rather than reflecting inherited enrichment signals from soil water evaporation in the watershed. Using a steady-state isotope mass balance analysis based on monthly ^{18}O and ^{2}H, we use the isotopic evolution of river water to re-construct a perspective of net exchange between the river and its contributing area along eight reaches of the river during a drought period from July 2002 to December 2003, including the duration of a minor flow event. The resulting scenario, which uses a combination of climatological averages and available real-time meteorological data, should be viewed as a preliminary test of the application rather than as a definitive inventory of reach water balance. As expected for a flood-driven dryland system, considerable temporal variability in exchange is predicted. While requiring additional real-time isotopic data for operational use, the method demonstrates potential as a non-invasive tool for detecting and quantifying water diversions, one that can be easily incorporated within existing water quality monitoring activities.

Keywords: Australia; Craig–Gordon model; Evaporation; Hydrogen-2; Oxygen-18; River water

1. Introduction

Australian water resources are especially vulnerable to climatic change and degradation due to a semi-arid climate and a high level of water development and utilisation in many areas. Research underway on the Darling River within the Australian Nuclear Science and Technology Organisation's (ANSTO) 'Isotopes for Water' Project has focused on refinement

*Corresponding author. Email: jjgibson@uvic.ca

Isotopes in Environmental and Health Studies
ISSN 1025-6016 print/ISSN 1477-2639 online © 2008 Taylor & Francis
http://www.tandf.co.uk/journals
DOI: 10.1080/10256010801887489

of isotope techniques including ^{18}O and ^{2}H for quantifying both natural and development-related impacts on the water cycle. These efforts, which form contributions to IAEAs global network for isotopes in precipitation (GNIP), IAEAs co-ordinated research project on large rivers, and to the Murray–Darling Basin GEWEX Project, include organisation of co-operative networks for monitoring ^{18}O and ^{2}H of groundwater, precipitation and evaporation pans as well as river discharge. To date, research in the Darling Basin has focused on a series of nine gauging stations (eight reaches) situated along the Barwon–Darling River System from Mungindi to Burtundy (figure 1), crossing a distance of over 1000 km, and stretching from the Queensland border to the Murray River confluence.

The basin drains an area of about 650,000 km^2, is characterised by very low gradients, and can be described as a dryland plain, with typically between 200 and 500 mm of annual precipitation and 2000 mm of potential evaporation along the main stem of the river. Flow along the main river stem below Mungindi station is highly dependant on episodic rainfall events in

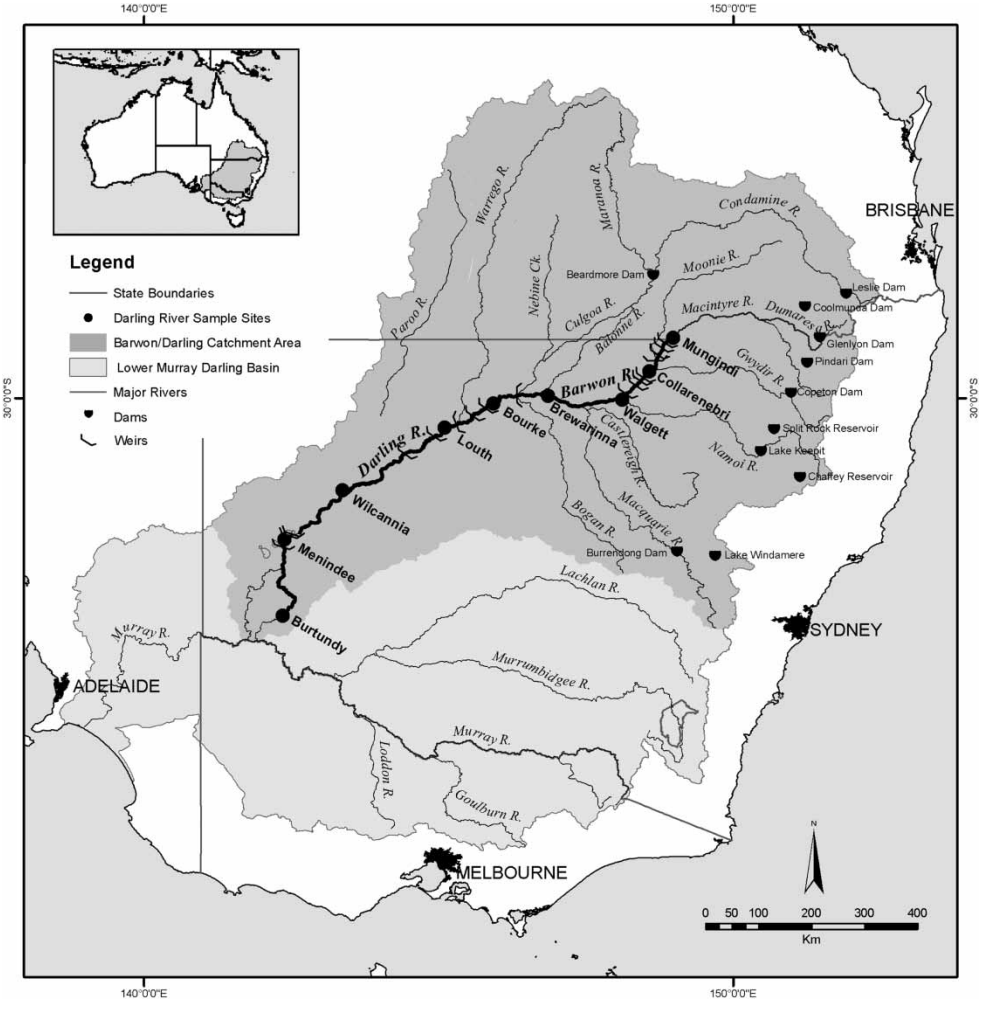

Figure 1. Map of Barwon–Darling River showing position of major weirs and control structures and location of water gauging and water sampling locations.

higher elevation and rainfall headwater catchments in the north and east of the basin and retains only a very muted natural seasonal maximum flow in summer, conspicuously overprinted by diversions and regulatory alterations. These headwater catchments contain 11 headwater dams with a full storage capacity of 4.6×10^9 m^3. Fifteen weirs control flow along the main Barwon–Darling river channel, which has 120 licensed water extractors, the majority of whom are situated along the Walgett to Bourke study reaches (reaches 3 and 4) (New South Wales State Water, M. Allen personal communication, 2007). Water licensees also include a significant number of diversion schemes to irrigate water-intensive crops, primarily cotton. In general, cotton growers and other agricultural users abstract and impound water opportunistically during times of flood, which has had a notable effect on the overall flux and timing of water discharge down the main stem of the river. The storage dams are generally shallow (<5 m) and between Mungindi and Wilcannia, the total storage capacity is $\sim 0.3 \times 10^9$ m^3 (New South Wales State Water, M. Allen personal communication, 2007). In 1997/98, diversions from the river accounted for an estimated 87 % of the long-term mean annual flow [1]. Although impacts have been generally described, more detailed temporal records of water diversions and water demand during hydrological events is desirable for improving sustainable management of the altered river ecosystem.

This paper describes a steady-state isotope balance method incorporating the Craig–Gordon [2] algorithm that shows considerable potential among many tested methodologies for tracing changes in the relative magnitude of gains and losses along river reaches during a representative drought–flood–drought cycle. The required sampling is easily incorporated within standard water quality monitoring programs and may therefore be well-suited to non-invasive audits of water balance evolution and diversion along this typical Australian dryland river. The approach relies on the quantitative evaporative enrichment in the stable, heavy isotopic species of water that occur in the river water during its residency in surface storage as described in the following section.

2. ^{2}H–^{18}O relationships

The isotope composition of the river is sensitive to hydrological perturbations because it is systematically enriched by evaporation above background levels in precipitation and groundwater. Water exchanges that occur as the river traverses the dryland region therefore cause measurable attenuation of the enrichment signal. A graphical comparison (figure 2) shows observed enrichment slopes in ^{2}H–^{18}O space to be similar to theoretically based values using weighted GNIP-based atmospheric moisture estimates [3].

High predictability is in part due to the river being primarily replenished by headwater basin inflows, with a lack of strong climatic gradients across the region. To a first approximation, the river acts as a series of semi-isolated, cascading water bodies with potential for groundwater exchange being limited by silt and clay deposits along the river floodplain, as well as potential for surface water inputs being reduced by the presence of thousands of weirs on tributaries and anabranches as well as farm dams within the reach catchments.

River water samples were collected and analysed for stable water isotopes (^{2}H and ^{18}O) beginning in July 2002. Isotopic data, combined with runoff discharge data [4], estimates of reach area from a comprehensive GIS analysis, and baseline monthly data from GNIP and nearby climate stations are used to evaluate the integrated gains and losses along the river, including a period of dynamic perturbations due to drought and flood conditions through a highly regulated, and agriculturally intensive, area as described quantitatively below.

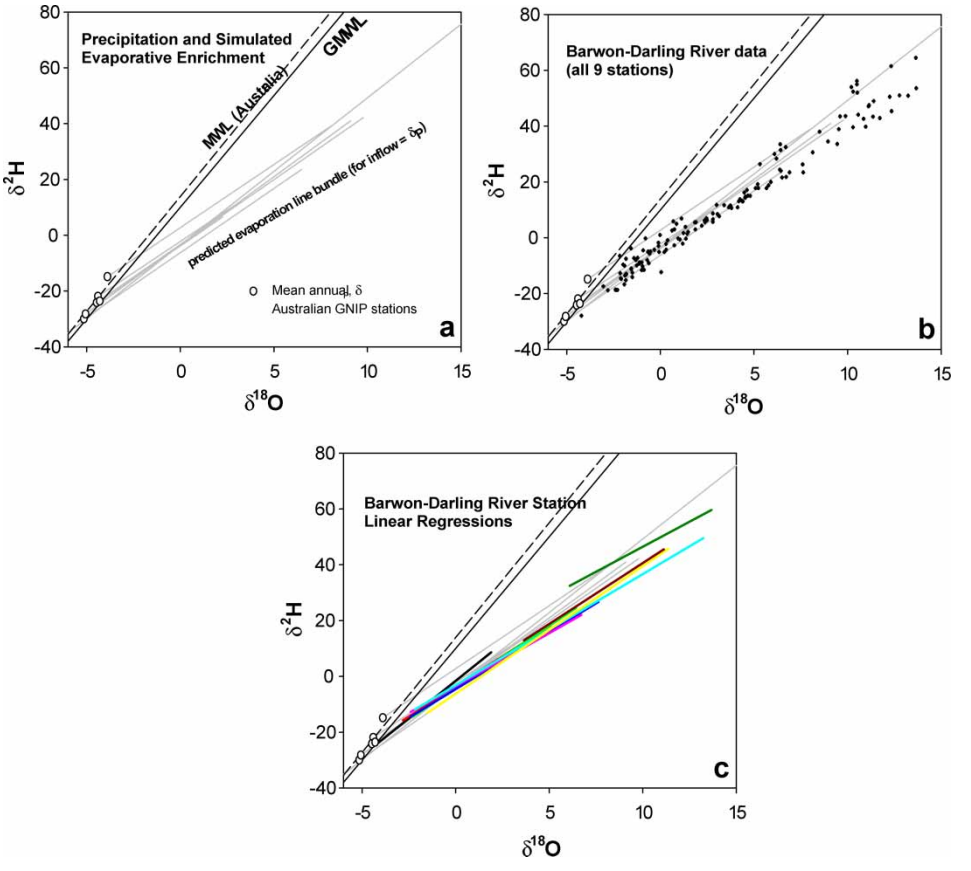

Figure 2. ^{2}H–^{18}O plots showing: (a) GNIP mean annual precipitation for Australian stations, and simulated evaporation lines for above based on an evaporation flux-weighting technique [3] and assuming an ideal precipitation-fed reservoir; (b) isotope composition of Barwon–Darling River discharge; and (c) linear regressions for individual sampling stations showing good agreement between observed and theoretical-predicted evaporation trends. In general, drought gradually enhances isotopic enrichment and flooding rapidly reduces it. Combined tracking of mass and isotope balance allows for independent assessment of ungauged inflows and outflows on the reach.

3. Method

A schematic of the isotope balance (figure 3) demonstrates the approach used to solve for net exchange (including separate characterisation of gains and losses) on a simple reach.

The model, ideally suited for evaporative systems where downstream isotopic changes are strongly driven by open-water evaporation and volumetric changes are limited, is used to test deviation from the initial working hypothesis that the river channel is substantially isolated from the watershed. The instantaneous mass and isotope balance for a river reach of volume V and isotope composition δ_V assuming hydrologic and isotopic steady-state, i.e. $dV/dt = 0$ and $d\delta_L/dt = 0$, respectively, are given by (figure 3)

$$I_R + I + P = Q + E, \tag{1}$$

$$I_R\delta_R + I\delta_I + P\delta_P = Q\delta_Q + E\delta_E, \tag{2}$$

where I is discharge at the upper gauging station on the reach, P is precipitation, Q is the discharge on the lower gauging station on the reach, E is evaporation on the reach, I_R is net water exchange on the reach and δ values are the isotope compositions of the respective

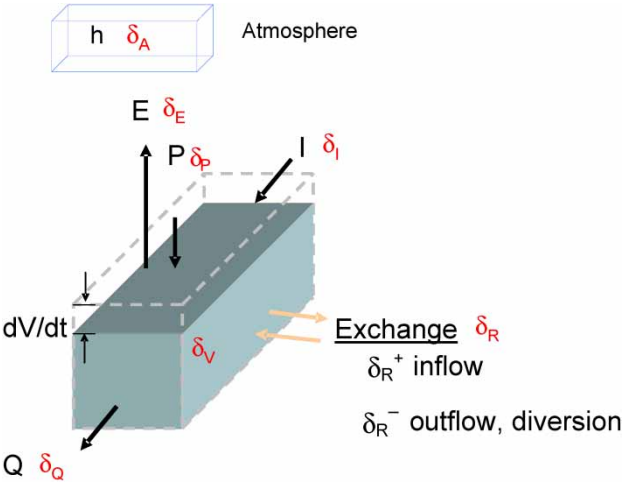

Figure 3. Steady-state reach balance analysis. Evaporative enrichment and climate data are used to estimate degree of potential exchange that is not recorded in the main river stem gauging network as inflow I and discharge Q.

fluxes. The gain/loss contributions to net exchange on the reach I_R can also be separately partitioned as $I_R = I_R^+ - I_R^-$, where I_R^+ is inflow from the reach catchment (i.e. tributary and groundwater inflow, irrigation return), and I_R^- is outflow to the reach catchment (i.e. recharge to groundwater, diversion). Substituting $I_R = I_R^+ - I_R^-$ into equations (1) and (2), respectively, yields

$$I_R^+ + I + P = I_R^- + Q + E, \tag{1a}$$

$$I_R^+\delta_R^+ + I\delta_I + P\delta_P = I_R^-\delta_R^- + Q\delta_Q + E\delta_E. \tag{2a}$$

The fraction of water loss by evaporation x_R, a primary control on evaporative isotopic enrichment on the reach, is calculated by combining equations (1a) and (2a) as

$$\begin{aligned} x_R &= \left(\frac{E}{(I_R^+ + I + P)}\right)_R \\ &= \frac{(I_R^+\delta_R^+ + I\delta_I + P\delta_P)/(I_R^+ + I + P) - (Q\delta_Q + I_R^-\delta_R^-)/(Q + I_R^-)}{\delta_E - (Q\delta_Q + I_R^-\delta_R^-)(Q + I_R^-)}. \end{aligned} \tag{3}$$

Assuming well-mixed conditions over discrete reaches, the liquid water stored on the reach is likely to have a similar isotopic composition to the gauged discharge, which is similar in turn to any net loss on the reach, i.e. $\delta_V \approx \delta_Q \approx \delta_R^-$. Also if water gains on the reach, a product of tributary inflow, irrigation returns and minor groundwater additions, are assumed to have a similar isotopic composition to upstream inflow, i.e. $\delta_R^+ \approx \delta_I$, then equation (3) can be simplified as follows:

$$x_R = \left(\frac{E}{I_R^+ + I + P}\right)_R = \frac{((I_R^+ + I)\delta_I + P\delta_P)/(I_R^+ + I + P) - \delta_Q}{\delta_E - \delta_Q}. \tag{3a}$$

Another useful hydrologic indicator is the cumulative evaporation loss that can be obtained by excluding all input apart from precipitation. In this case, an equivalent expression to

equation (3) can be written for cumulative water loss by evaporation for a river gauging station

$$x_c = \left(\frac{E_w}{P_w}\right)_C = \frac{\delta_P - \delta_Q}{\delta_E - \delta_Q}, \tag{3b}$$

where E_w and P_w are the cumulative evaporation loss and precipitation from the flux-weighted contributing areas of the watershed.

From a conventional water balance perspective, equation (1) allows for estimation of the net exchange on the reach. For systems with a significant evaporative enrichment signal, as is the case for the Darling River and many dryland river systems, isotopic characterisation of the various reach components in a well-gauged system also enables the partitioning of the net exchange. Essentially, the isotope balance assumes that all vapour losses are via open-water evaporation that is isotopically fractionating, but does not assume that $(I + P)$ and Q, respectively, reflect the total liquid inflow and outflows from the system. The gaining contribution to the net exchange on the reach is then estimated from equation (3a) as

$$I_R^+ = \frac{E - x_R(I + P)}{x_R} \tag{4}$$

and the losing contribution to net exchange on the reach, given that $(Q + I_R^-)/(I_R^+ + I + P) = 1 - x_R$, is evaluated as

$$I_R^- = (1 - x_E)\left(I_R^+ + I + P\right) - Q, \tag{5}$$

A schematic representation (figure 3) illustrates the major fluxes and their isotopic compositions for a simple reach. Note that the isotope composition of the evaporation flux, δ_E, is difficult to measure directly, can be indirectly estimated using a commonly used form [5] of the Craig–Gordon turbulent diffusion model [2]:

$$\delta_E = \frac{\alpha^{+-1}\delta_L - h\delta_A - \varepsilon}{1 - h + 10^{-3}\varepsilon_K}, \tag{6}$$

where $\alpha^+ > 1$ is the equilibrium liquid–vapour isotope fractionation, h is the atmospheric relative humidity (expressed as a decimal fraction ranging from 0 to 1, δ_A is the isotopic composition of ambient moisture, and $\varepsilon = \varepsilon^* + \varepsilon_K$, where ε is the total isotopic separation factor comprising both equilibrium ε^* and kinetic ε_K contributions. Equilibrium separation factors ε^* for oxygen and hydrogen, which vary with temperature, are adopted from laboratory experiments of Horita and Weslowski [6]. Kinetic separation factors ε_K were approximated based on Gat [5] as $\varepsilon_K = C_K\theta(1 - h)$, where $C_K = (D/D_i)^n - 1$ and D is the molecular diffusion co-efficient of $^1H_2{}^{16}O$, D_i is the molecular diffusion co-efficient of $^1H_2{}^{18}O$ or $^1H^2H^{16}O$, θ an advection term assumed herein to be 1, implying that the river has little impact on the ambient moisture composition, and $n = 1/2$ is used signifying fully turbulent, open-water exchange. This results in C_K of close to 14.3 % and 12.5 % for oxygen and hydrogen, respectively, values widely used to describe evaporation from open-water bodies [7].

Note that this approach is not able to distinguish transpiration loss and liquid outflow, which are both isotopically non-fractionating [5], so that I_R^- will be overestimated in cases where transpiration losses from riverine wetlands or vegetated near-channel margins of the river are significant.

The runoff ratio for a reach catchment can also be estimated from the isotope balance and precipitation data using

$$R_r = \frac{I_R^+}{P_{Rw}}, \tag{7}$$

where P_{Rw} is the volume of precipitation falling on the reach watershed area.

Table 1. Summary of physical properties by river reach.

Reach	Channel length (10^5 m)	Meander co-effecient†	Channel width (m)		Mean area (10^6 m^2)	Storage volume (10^6 m^3)	Inflow range (10^6 m^3/month)			Residence time based on inflow range (month)			Reach catchment area (10^3 km^2)
			Mean max	Mean min			Mean	Mean + 1std	Max	Mean	Mean + 1std	Max	
1	1.2	1.61	32.5	28.3	3.7	5.5	11	29	70	0.5	0.2	0.08	41.4
2	1.1	1.48	24.9	21.1	2.6	3.9	12	33	89	0.3	0.1	0.04	46.7
3	2.5	1.9	28.5	24.8	6.6	9.9	11	29	75	0.9	0.3	0.1	197
4	1.9	1.85	44.3	39.7	7.8	12	10	26	61	1.2	0.5	0.2	57
5	1.9	1.88	49.6	41.3	8.6	13	7	20	38	1.9	0.7	0.3	103
6	4.2	2.1	30.6	17.7	10.2	15	6	17	42	2.5	0.9	0.4	80.5
7	2.8	2.27	12.4	5.1	2.5	3.7	2	4	5	1.9	0.9	0.7	5.2
8	3.2	2.16	11.1	5.4	2.7	4	2	3	5	2.0	1.3	0.8	72.2
Total	18.8				44.6	67				11.0	5.0	3.0	603

†Inter-station distance/channel length.

4. Data used in the model

The isotope balance model incorporates monthly gauge data obtained along the main stem of the Barwon–Darling River System as well as a GIS analysis of reach surface and catchment areas (table 1) and precipitation, evaporation, temperature and humidity data interpolated from nearby climate stations (table 2, figure 4). To simply account for lags during river routing, isotopic measurements were assumed to be representative of the previous months' flow and atmospheric conditions at all time steps for all stations.

Although transit time of the system is not exactly one month, the summary provided in table 1 suggests average residence times of between 0.3 and 2 months, averaging about 1.4 months under average flow conditions, with shorter residence times during peak flow. While this approach is not a substitute for a rigorous routing model, the sluggishness of the system seems fortuitously to lend itself to this kind of simplification, one that seems adequate at this preliminary stage to demonstrate the capability of the method. Of course, more dynamic periods are therefore not expected to be as accurately captured. An obvious future improvement would be to integrate the isotope balance calculations within a numerical river routing model to capture real-time variation in transit time, although this is beyond the scope of this paper.

For the analysis, monthly river isotopic data and volumetric data were obtained at nine stations along the river course and are used to define the input and output to eight river reaches. Depth equivalents of evaporation and precipitation in millimetre/month (figure 4b) were converted to volumes based on time series of the reach area over the course of the study period (figure 4c). These trends (figure 4) generally depict the climatic gradients along the course of the river.

The isotopic composition of precipitation and groundwater are assumed to be similar and invariant, and are assumed to lie along the meteoric water line at the intersection of the local evaporation line (figure 2) with a δ^{18}O value of $-4\,\%$. This assumption is consistent with the Australian GNIP data and with understanding of the local hydrology, i.e. that recharge occurs predominantly by infiltration of heavy rains. The isotopic composition of atmospheric moisture was determined using the flux-weighted algorithm [3] based on the nearby GNIP

Table 2. Climatic stations used in the interpolation analysis.

OID	Station	Long	Lat
1	Mungindi	148.9899	−28.9786
2	Collarenebri	148.5818	−29.5407
3	Walgett	148.1218	−30.0236
4	Brewarrina	146.8651	−29.9614
5	Bourke	145.9358	−30.0917
6	Wilcannia	143.3747	−31.5631
7	Menindee	142.4173	−32.3937
8	Lake Victoria	141.2769	−33.9890
9	Wentworth	141.9187	−34.1066
10	White Cliffs	143.0897	−30.8506
11	Broken Hill	141.5930	−31.8803
12	Cobar	145.8341	−31.4968
13	Moree	149.8383	−29.4819
14	Narrabri	149.7552	−30.3401
15	Yarras	152.2482	−31.3865
16	Gilruth Plains	145.9833	−28.1000
17	Thargomindah	143.8197	−27.9978
18	Inglewood	150.9333	−28.5000
19	Goodooga	147.4543	−29.1142

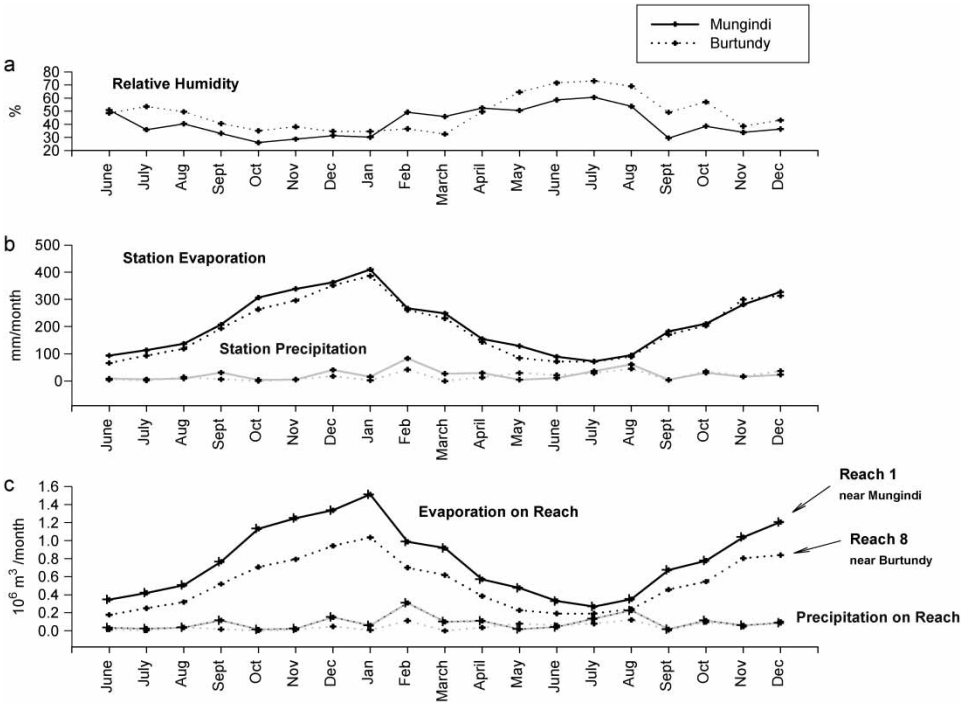

Figure 4. Example of climate-driven parameters used in the isotope balance model showing range of conditions for stations located upstream (Mungindi, solid line) and downstream (Burtundy, dotted line), including: (a) monthly relative humidity (%); (b) station evaporation and precipitation; and (c) evaporation and precipitation for reach 1 near Mungindi (solid line) and reach 8 near Burtundy (dotted line).

data and climatology, but is found to reasonably replicate the slope and degree of enrichment observed along the course of the river (figure 2). In future, use of evaporation pans at climate stations along the reaches will be tested to improve real-time variability of the atmospheric moisture using the method of Gibson *et al.* [8].

The reach storage is modelled as being isotopically uniform and well mixed so that water losses are considered to be compositionally similar to the discharge. Importantly, the presence of many water level control structures along the various reaches tends to limit the total volumetric storage changes on the reaches, except during extremely wet and dry periods, so that the system has a tendency to remain at near hydrologic steady-state for long periods. Water gains were assumed to be a mixture of groundwater, with similar isotopic characteristics to precipitation, and upstream river water (as would be the case for irrigated water being diverted upstream and returned downstream on the reach). The isotope signature of this precipitation-inflow mixture was dynamically computed within the model and simultaneously solved along with the reach water exchanges. Periods for which river isotope data were missing are not evaluated.

5. Results

Isotopic results and derived E/I estimates are shown in figures 5b and 5c, respectively and ungauged inflow, ungauged outflow and net exchanges are summarized in figures 6a through 6c, respectively. Derived runoff ratios (figure 7) are provided separately for upper, middle

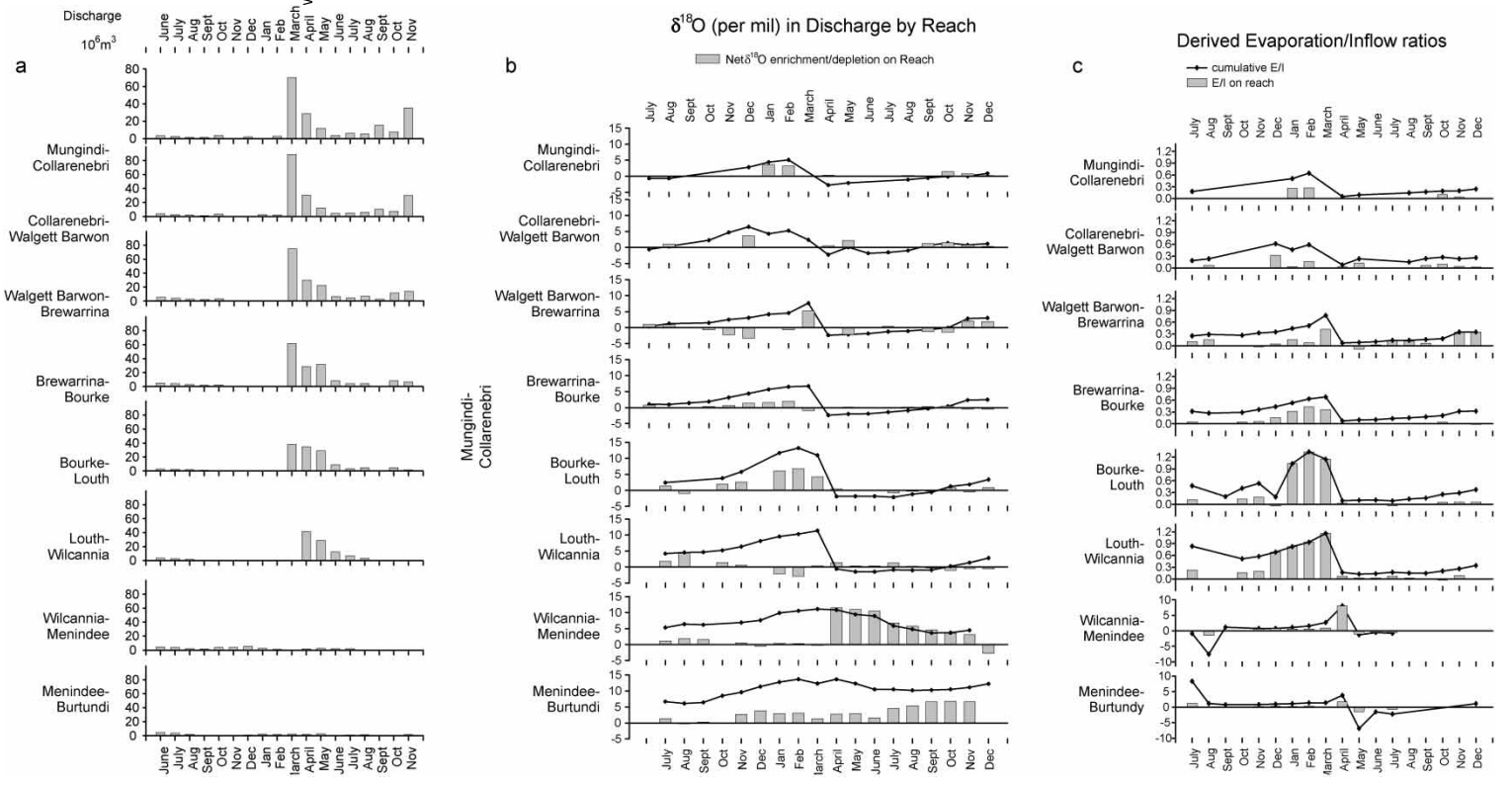

Figure 5. Time series of: (a) gauged discharge (m^3/month); (b) $\delta^{18}O$ in discharge and net enrichment; and (c) cumulative evaporation loss and evaporation loss on the reach during June 2002–December 2003.

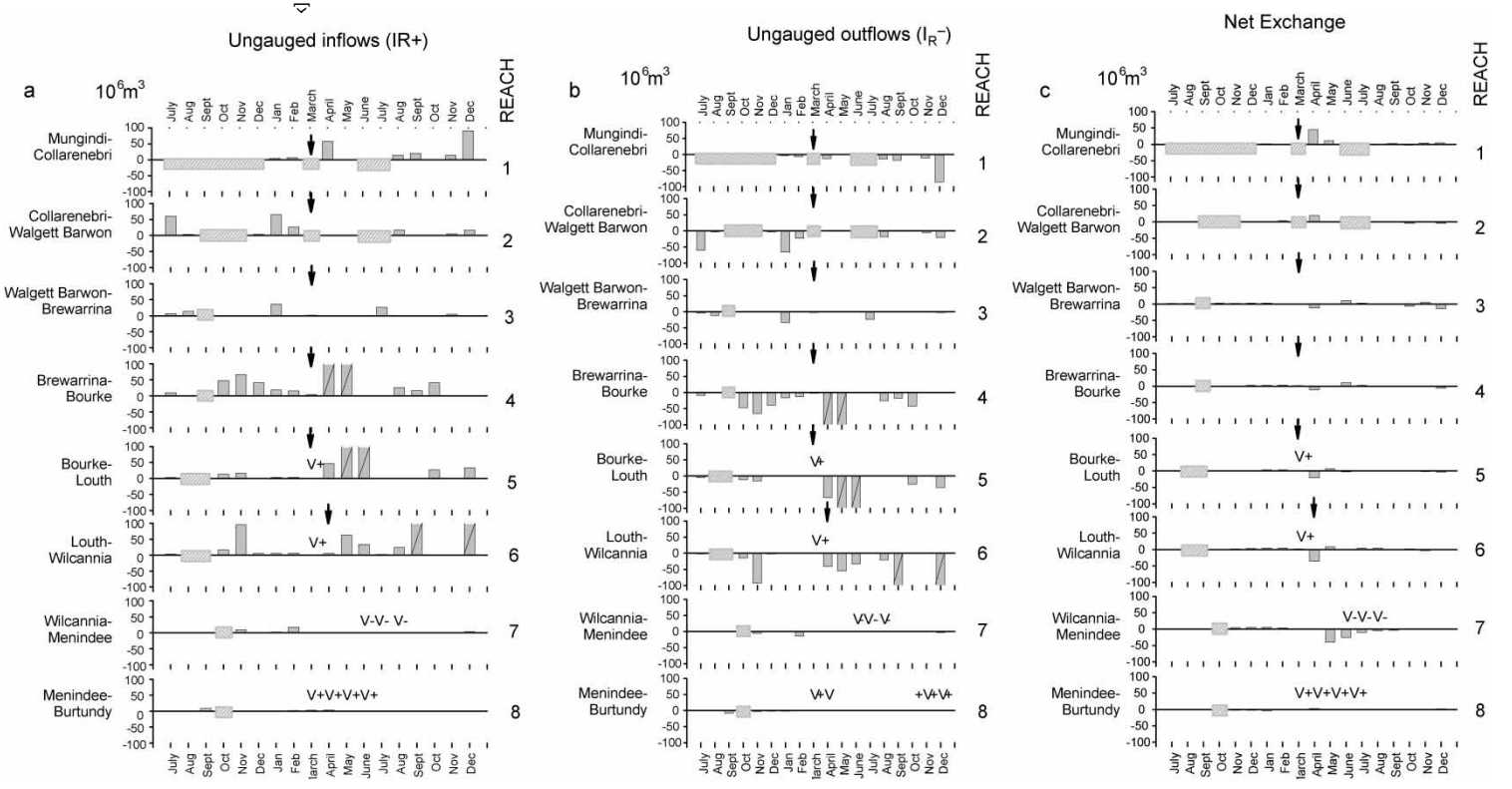

Figure 6. Monthly time series of ungauged inflows (a) outflows; (b) and net exchange (m^3); (c) on reaches of the Darling River predicted by isotope balance. Hatched grey boxes denote months when determinations were not made due to missing information (23 of 144 reach-months). Overall, water gains are predicted for 65 % of cases evaluated. Fluxes greater than 2×10^8 m^3/month are indicated to be offscale by cross hatched bars. Note that V− denotes apparent evaporative drawdown of the river reach and V+ suggests significant volumetric gain. Timing of the main flow pulse on each reach is shown as downward arrows. Outlines depict gradual declines in inflow before the flow event on some reaches.

Table 3. Example of model inputs for the isotope mass balance model, January 2002.

January 2002	Hydrometric and isotopic data											
Reach balance	Q (m^3)	δ_Q	I (m^3)	δ_I	P (m^3)	δ_P	E (m^3)	h	T	$I + P$ (m^3)	δ_R	Enrich on reach
First reach	2,012,640	4.38	1,689,250	0.74	150,081	−4	1,336,223	0.31	20	1,839,331	0.353238	3.64
Second reach	528,970	4.25	2,012,640	4.38	105,521	−4	952,874	0.28	20	2,118,161	3.962531	−0.13
Third reach	343,500	4.13	528,970	4.25	119,624	−4	2,460,585	0.27	20	648,594	2.728404	−0.12
Fourth reach	0	5.67	343,500	4.13	92,604	−4	3,003,175	0.22	20	436,104	2.403648	1.54
Fifth reach	0	11.72	0	5.67	49,255	−4	3,197,993	0.22	20	49,255	−4	6.05
Sixth reach	39780	9.53	0	11.72	85,993	−4	3,743,475	0.23	20	85,993	−4	−2.19
Seventh reach	5,457,970	9.89	39,780	9.53	34,022	−4	899,880	0.29	20	73,802	3.292825	0.36
Eigth reach	902,480	12.77	5,457,970	9.89	47,691	−4	941497.7	0.35	20	5,505,661	9.769682	2.88

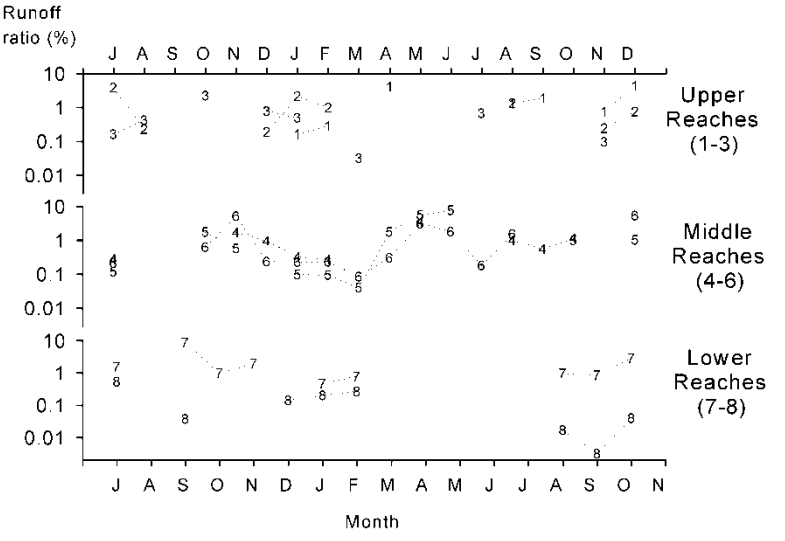

Figure 7. Derived runoff ratios by month (I_R^+/P, $m^3/m^3 \times 100\,\%$) based on isotopic estimates of ungauged inflow over the reach catchments.

Table 4. Example of internal calculations for the isotope mass balance model, January 2002.

January 2002	Internal isotope calculations				
Reach balance	δ_A	ε^*	ε_K	m	δ^*
First reach	−13.55	0.0096	0.0098	0.422	51.21
Second reach	−13.55	0.0096	0.0103	0.349	62.83
Third reach	−13.55	0.0096	0.0104	0.332	66.29
Fourth reach	−13.55	0.0096	0.0111	0.252	88.52
Fifth reach	−13.55	0.0096	0.0110	0.257	86.59
Sixth reach	−13.55	0.0096	0.0110	0.260	85.64
Seventh reach	−13.55	0.0096	0.0101	0.371	58.90
Eigth reach	−13.55	0.0096	0.0093	0.491	43.47

m is enrichment slope, defined in [8].

Table 5. Example of model outputs for the isotope mass balance model, January 2002.

January 2002	Model output				
Reach balance	Reach E/I	Cumulative E/I	Calculated I_R	Calculated I_R^-	Calculated I_R^+
First reach	0.20	0.42	1.5E + 06	3.2E + 06	4.7E + 06
Second reach	0.02	0.40	−6.4E + 05	6.6E + 07	6.6E + 07
Third reach	0.07	0.39	2.2E + 06	3.3E + 07	3.6E + 07
Fourth reach	0.16	0.46	2.6E + 06	1.6E + 07	1.9E + 07
Fifth reach	0.82	0.82	3.1E + 06	7.2E + 05	3.9E + 06
Sixth reach	0.68	0.68	3.7E + 06	1.7E + 06	5.4E + 06
Seventh reach	0.36	0.76	6.3E + 06	(3.9E + 06)†	2.4E + 06
Eigth reach	0.20	1.11	−3.7E + 06‡	2.9E + 06	(7.8E + 05)‡

†Ungauged outflow is negative; this condition suggests that the model may not be performing optimally due to significant volumetric gains on reach.
‡Total inflow and ungauged inflows are negative; this condition and $E/I > 1$ suggests that the model may not be performing optimally due to significant volumetric losses on reach.

and lower reaches. An example of inputs, outputs and internal calculations made within the isotope balance model for a selected time step (January 2002) are also included to clarify the basis of the approach for the reader (tables 3–5). Note that ungauged inflows and runoff ratios reflect all sources of inflow along the reach from the reach catchment including tributary inflow, irrigation return flows and groundwater. Ungauged outflows include water losses to abstraction for water supply and irrigation, floodplain recharge and interaction (known to be negligible during the study period), riverbank infiltration, anabranch replenishment and groundwater losses. Note that runoff ratios only reflect water that reaches the main stem of the river and therefore excludes diversions to tributary weirs, farm dams or other interception schemes.

6. Discussion

The main stem physical monitoring data alone, that is, the discharge (figure 5a) and reach net exchange (figure 6c) suggest an orderly, slow draining river system with very little exchange of water between channel, floodplain, anabranches and groundwater reservoirs. However, the isotopic composition of water and derived E/I estimates (figures 5b and 5c, respectively) at times reveal a more complex, dynamic hydrologic balance on some reaches with apparent influx and outflux of ungauged water required to account for the isotopic evolution of water along the various reaches. Derived E/I ratios (figure 5c) clearly depict the progressive trend toward more evaporative conditions and lower throughflow on reaches during July 2002 through March 2003. Resetting of the isotopic enrichment signals and E/I after the March flow event is also evident, followed by progressive heavy isotope enrichment recording E/I increases from April 2003 until the record ends in December 2003. Water exchanges (figure 6) based on the E/I ratios and isotope balance further illustrate the occurrence of dynamic temporal exchanges along the reaches.

The reach isotope balance approach essentially enables removal of the evaporation, precipitation and upstream input effects and was found to be a reliable diagnostic for quantifying the temporal pattern of net gains along the river course from other sources (i.e. tributary input, groundwater inflow and irrigation return), net losses to the river (i.e. groundwater outflow, overbank flooding or irrigation diversion) and occurrence of strongly evaporative situations leading to volumetric reduction. Not surprisingly, the analysis reveals that the river is never totally isolated from its catchment. Four reaches of the river (reaches 1 and 4 through 6) were found to be volumetrically gaining reaches, whereas the remainder were losing reaches. Major water losses on losing reaches are attributed to diversion of water for agriculture (reaches 2–3) and to the Menindee lakes scheme (reaches 7–8). It is important to note that ungauged outflow losses on all reaches likely include some transpiration losses from trees tapping into river water sources along the floodplain, although the magnitude of this flux is unknown and is currently undifferentiated in the summary.

For 51 % of all reach-months evaluated between July 2002 and December 2003, it appears that the river was gaining water along its course. About 8 % of the time-calculated E/I ratios were negative or greater than one, suggesting changes in volume that evidently violated the hydrologic steady-state approximation. For 5 % of cases, mostly very dynamic flooding intervals, estimated inflows were considered to be unreasonably large ($>10^8$ m^3) and these are shown as hatched bars in figure 6. As a result, quantitative estimates are very approximate and should be viewed cautiously beyond indication of gain or loss. Overall, the most dynamic reaches in terms of exchange are reaches 4 through 6, and the reaches most affected by volumetric changes are reaches 7 and 8 (Wilcania to Burtundy).

One of the major sources of inflow to the main stem, particularly along reach 2 through 6 during October–December 2002, on reach 1 during August–December 2003 and reach 4 during August–October 2003, is storm flow derived from tributary headwaters. According to ungauged outflow estimates, these waters are apparently diverted or abstracted almost entirely along the same reaches. The practice of allowing diversion of water on the Darling based on weir gauge height thresholds is consistent with these findings. The potential value-added with isotope monitoring in this case is that lower-than-expected isotopic enrichment on a reach can be used to trace the occurrence of high-throughflow reaches suggestive of water exchanges that would otherwise go undetected by the main-stem gauging network. In future, further discrimination of the specific causes of throughflow anomalies could be gleaned by accounting for all gauged tributary inflows on each reach as well as all licensed extractions. More effort on this is warranted when more complete real-time datasets are available and can be integrated within a river routing model.

It is known that abstraction and diversion of water, particularly for cotton growing and other agricultural activities is generally conducted during times of peak flows along the main stem of the Barwon–Darling System. The flow event recorded here reached Mungindi in March 2003, with the flow peak propagating downstream to Wilcannia within about 1 month (see downward arrows, figure 6). Diversion of water in the months following the high-flow episode is evident particularly on reaches 4 through 6 (figure 6b). While a more detailed analysis is required to carefully verify the quantities of water exchange by type, a preliminary assessment of monthly runoff ratios for the reach catchments suggests that the total inflow estimates are reasonable (figure 7).

Runoff ratios, evaluated as inflow/precipitation, were found to range upwards to 5.7 %, with the majority of values lying in the 0.1–1 % range. Such values, and coherent declines in the calculated net runoff for some reaches during periods of extended drought, are consistent with expected runoff patterns for a dryland system. Further development of the isotopic approach and isotopic characteristics of the system including isotopic composition of groundwater is expected to improve capability for evaluating compliance with water licensing regulations, for examining human/agricultural impacts on flooding and for improving future water allocation schemes in the basin.

7. Future studies

Isotope mass balance of the Barwon–Darling System is part of an ongoing research program of ANSTOs Isotopes for Water Project involving physical, isotopic and geochemical investigations aspects of which have been carried out in collaboration with the Bureau of Meteorology, CSIRO and DNR. One important avenue of future research is to better define the real-time atmospheric controls on isotopic enrichment by monitoring isotopic composition of evaporation pans in conjunction with monthly precipitation monitoring within the Australian GNIP network in the region. Better isotopic characterisation of groundwater storages along the river floodplain and coupled use of isotopic and geochemical tracers such as chloride are promising directions being explored to further partition water losses due to transpiration from liquid outflows, which are not readily separable in the present context with isotope tracers alone.

Acknowledgements

The authors would like to thank NSW Department of Natural Resources for their in-kind support for this project, particularly in providing water samples for isotopic analysis.

References

[1] M.C. Thoms, F. Sheldon. Water resource development and hydrological change in a large dryland river: the Barwon–Darling River, Australia. *J. Hydrol.*, **228**, 10–21 (2000).

[2] H. Craig, L.I. Gordon. Deuterium and oxygen-18 variations in the ocean and marine at mosphere. In *Stable Isotopes in Oceanographic Studies and Paleotemperatures*, E. Tongiorgi (Ed.), pp. 9–130, Lab. Geologia Nucleare, Pisa (1965).

[3] J.J. Gibson, S.J. Birks, T.W.D. Edwards. Global predictions of δ_A and δ^2H and δ^{18}O evaporation slopes: evaluating the importance of seasonality. *Global Biogeochem. Cycles*, in press.

[4] DNR 2007. *PINNEENA 9*, *New South Wales Surface Water Data Archive*, NSW Department of Natural Resources (2007).

[5] J.R. Gat. Oxygen and hydrogen isotopes in the hydrological cycle. *Annu. Rev. Earth Planet. Sci.*, **24**, 225–262 (1996).

[6] J. Horita, D. Wesolowski. Liquid–vapour fractionation of oxygen and hydrogen isotopes of water from the freezing to the critical temperature. *Geochem. Cosmochim. Acta*, **47**, 2314–2326 (1994).

[7] R. Gonfiantini. Environmental isotopes in lake studies. In *Handbook of Environmental Isotope Geochemistry*, Vol. 3, P. Fritz, J.Ch. Fontes (Eds), pp. 113–168, Elsevier, New York (1986).

[8] J.J. Gibson, T.W.D. Edwards, T.D. Prowse. Pan-derived isotopic composition of water vapour and its variability in northern Canada. *J. Hydrol.*, **217**, 55–74 (1999).